Available online at www.sciencedirect.com

SCIENCE DIRECT®

Catalysis Today 96 (2004) 161–164

CATALYSIS TODAY

www.elsevier.com/locate/cattod

Synthesis, characterization and application of nano-structured Mo_2C thin films

H.Y. Chen[a], L. Chen[a], Y. Lu[a], Q. Hong[a], H.C. Chua[b], S.B. Tang[b], J. Lin[b,*]

[a] *Chemical & Process Engineering Center, National University of Singapore, Singapore 119260, Singapore*
[b] *Department of Physics, National University of Singapore, Singapore 119260, Singapore*

Abstract

Nano-structured Mo_2C thin films were grown on Si(1 0 0) by metal-organic chemical vapor deposition using $Mo(CO)_6$ as precursor. Well crystalline thin films could be synthesized only in the case where the precursor vapor was present before deposition temperature was rapidly reached. A reaction scheme is postulated. The formation of benzene from methane over the nano-structured Mo films has been observed in micro-reactor studies and confirms that $Mo_2C + MoO_3$ are an active catalyst for methane conversion.

Keywords: Nano-structure; Thin films; MOCVD; Mo_2C; $Mo(CO)_6$

1. Introduction

Recently, nano-scale materials are receiving a great deal of interest owing to their unique character and potential applications [1–4]. In the research of methane activation, Mo_2C is recognized as an intermediate or active material, responsible for methane conversion to aromatics [5–7]. Unfortunately, there has been still a lack of convincing evidence and detailed explanation of the function of Mo_2C in the Mo-based catalyst system for methane aromatization. In this paper, a nano-structured Mo_2C catalyst was synthesized using metal-organic chemical vapor deposition (MOCVD), and characterized by SEM, XPS, AES and XRD. The application of these nano-structured Mo films as catalyst for methane conversion was also investigated in a micro-reactor study.

2. Experimental

Mo_2C thin films were prepared in a home-made CVD device equipped with a rapid-heating RF induction furnace (Fig. 1). Si(1 0 0) was used as the substrate, and $Mo(CO)_6$ as MOCVD precursor. The deposition was conducted in the reactor by maintaining the pressure of the organo-metallic $Mo(CO)_6$ at 2×10^{-1} mbar while rapidly heating the substrate to the desired temperature within 15 s. The deposition time was optimized and controlled to achieve nano-structured thin films in less than 120 s.

XPS and AES analysis were carried out in VG ESCALAB MKII, using a Mg Kα X-ray source (1253.6 eV, 150 W) at a constant analyzer pass energy of 20 eV for XPS. The spectra were normally recorded at take-off angles (photoelectron detection angle with respect to the film surface) of 20° and 75°, respectively, in order to compare data obtained from different sampling depths. Sample charging was corrected for by referencing to adventitious C 1s at a binding energy 284.6 eV.

3. Results and discussion

3.1. Thin film growth of nano-structured Mo_2C/MoO_3

Two deposition modes were explored for the film growth. In mode 1, the desired deposition temperature was reached before introducing the precursor, whereas in mode 2, the sample was rapidly heated to the deposition temperature in the presence of a precursor atmosphere. The detailed conditions are listed in Table 1. As revealed by SEM (Fig. 2), nano-structured thin films form only under mode 2 conditions.

---

[*] Corresponding author. Tel.: +65-8742616; fax: +65-7776126.
E-mail address: phylinjy@nus.edu.sg (J. Lin).

0920-5861/$ – see front matter © 2004 Elsevier B.V. All rights reserved.
doi:10.1016/j.cattod.2004.06.116

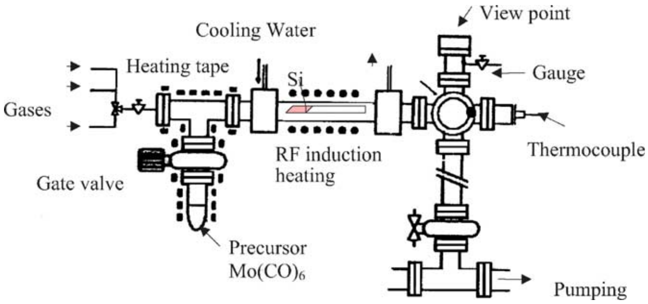

Fig. 1. The schematics of MOCVD set-up equipped with rf induction heater.

Obviously, the key step to obtain nano-structured thin films is the rapid heating of the substrate in the presence of $Mo(CO)_6$. This is probably because the rapid temperature rise at the initial deposition stage may result in the formation of small seed particles, and thereafter, the high temperature facilitates the growth of nano-structured thin films. Our experiments showed that conventional resistance heating cannot bring about the formation of these nano-structured thin films, in agreement with earlier observations [8]. The experimental results also indicated that a higher deposition temperature or a rapid annealing process is favorable to the formation of molybdenum carbide (see Table 1). As reported in literature [9], molybdenum hexacarbonyl has been widely used in the growth of Mo films at temperature of ~300 °C with the reaction shown below:

$$Mo(CO)_6 \rightarrow Mo + 6CO$$

Thus, it is understandable that the formation of Mo_2C could be due to the reaction of CO and Mo at higher temperatures. The presence of MoO_3 in the films was also confirmed by XPS and XRD. Its formation may result also from the reaction between Mo and CO [10]. The reaction scheme can be postulated as follows:

$$2CO \rightarrow C + CO_2$$

$$2Mo + C \rightarrow Mo_2C$$

$$7Mo + 3CO \rightarrow 3Mo_2C + MoO_3$$

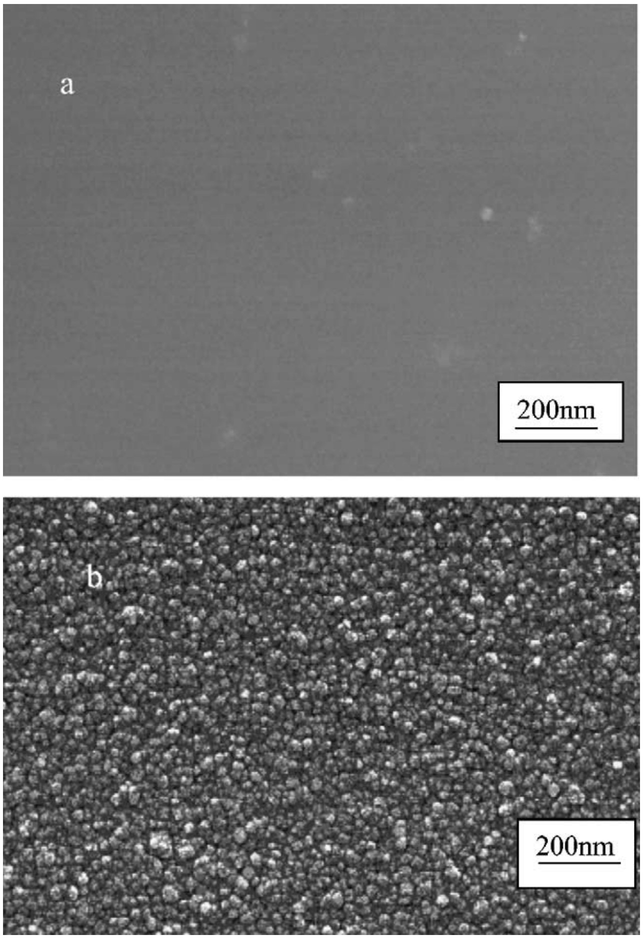

Fig. 2. Field emission SEM images taken from thin films grown at 600 °C with the processes of (a) mode 1 and (b) mode 2.

3.2. Surface characterization of thin films by XPS and AES

Fig. 3 shows a typical XPS wide scan of the film grown under mode 2 conditions, showing mainly carbon, oxygen and molybdenum on the surface. The silicon peaks could not be detected, as the film was thicker than 10 nm.

Table 1
Growth condition and chemical composition of grown films

Substrate	Deposition vapor pressure (mbar)	Deposition temperature (°C)	Surface species mol% (determined by XPS)
Mode 1			
Si(1 0 0)	5×10^{-1}	250	100% MoO_3
Si(1 0 0)	5×10^{-1}	400	50% Mo, 50% MoO_3
Si(1 0 0)	5×10^{-1}	600	58% Mo_2C, 42% MoO_3
Si(1 0 0)	5×10^{-1}	600 (calcined at 1000)	73% Mo_2C, 27% MoO_3
Si(1 0 0)	5×10^{-1}	700	86% Mo_2C, 14% MoO_3
Mode 2			
Si(1 0 0)	2×10^{-1}	400	52% Mo, 48% MoO_3
Si(1 0 0)	2×10^{-1}	400 (calcined at 1000)	62% Mo_2C, 38% MoO_3
Si(1 0 0)	2×10^{-1}	600	84% Mo_2C, 16% MoO_3
Si(1 0 0)	2×10^{-1}	600 (calcined at 1000)	86% Mo_2C, 14% MoO_3

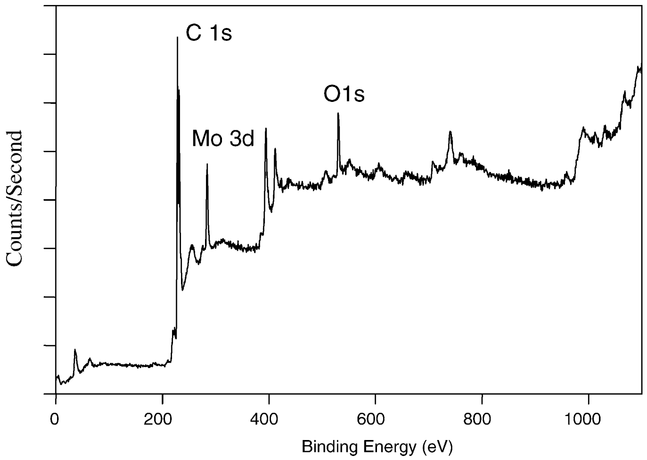

Fig. 3. XPS wide scan for thin film grown at 600 °C, 120 s.

Mo 3d narrow scans are presented in Fig. 4 for the two samples obtained at different deposition temperatures. Spectrum (a) for the film grown at 400 °C shows a peak located at BE 228.5 eV which is due to Mo^0, while that at 232.6 eV is due to a Mo^{6+} oxide species, indicating that the film surface is composed of Mo and MoO_3. Trace (b) from a film grown at 600 °C shows the Mo 3d peak at BE 227.8 eV which can be attributed to a Mo carbide species. This assignment is corroborated by the presence of the corresponding carbide C 1s at BE 282.7 eV. A small amount of a MoO_3 species is also present.

An AES depth profile was obtained to investigate the distribution of the various species throughout the film. The profile in Fig. 5 shows that the film is very homogeneous. It indicates that the concentrations of the Mo, C and O species are almost constant throughout the entire thickness of the film. The sudden appearance of the Si after prolonged sputtering indicates a sharp interface between the film and the Si substrate. The average atomic ratio of Mo to C is approximately 4:1, indicating that the film consists mainly of molybdenum metal and Mo_2C, with a small amount of MoO_3.

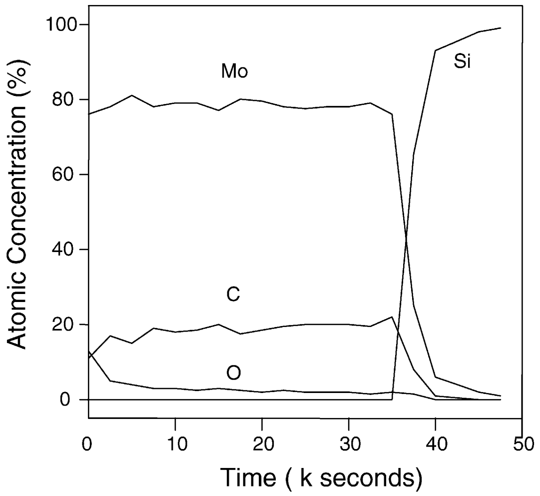

Fig. 5. AES depth profile of the thin film showing the atomic concentration percentage against the etching time.

From Auger depth profiles, the thickness of the film after a deposition time of 120 min was approximately 320 nm (based on the sputtering condition: 5 kV Ar^+ ion, 5×10^{-8} mbar partial pressure, the sputtering rate on Ta_2O_3 standard is 5 A/min and spatial resolution 2000 Å).

XRD was also used to analyze the film. Typically, diffraction lines could be observed at $2\theta = 29^\circ$ (strong) and 49° (doublet). From the JCPDS XRD data files [11], the peak at 29° was identified as $Mo_2C(2\,2\,0)$ while that at 49° is due to the reflection from $MoSi_2(1\,1\,2)$.

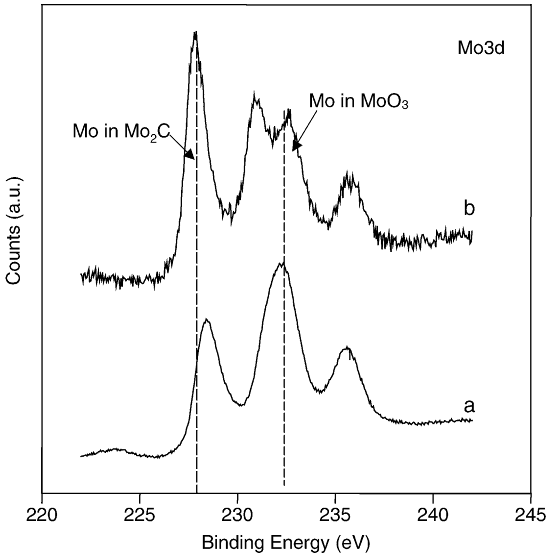

Fig. 4. Mo 3d XPS core level spectra obtained from the films grown at (a) 400 °C and (b) 600 °C with rapid temperature ramp.

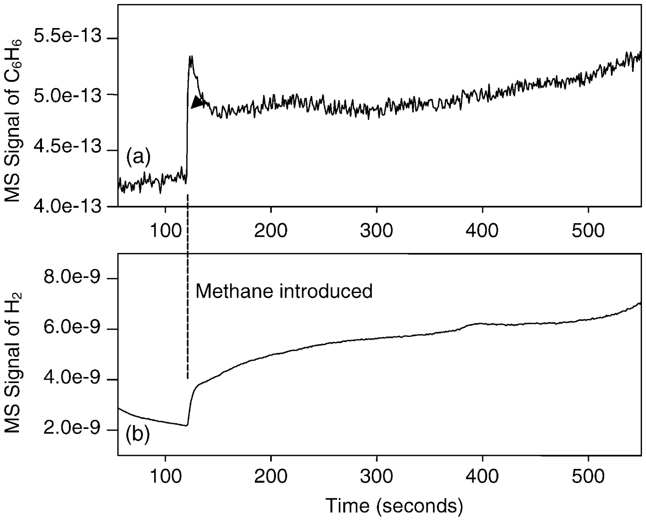

Fig. 6. On-line MS profiles monitoring (a) benzene and (b) hydrogen mass ion current against the reaction time (data acquisition cycles) in CH_4 stream at 700 °C.

3.3. Catalytic activity of Mo_2C thin films in methane aromatization

As Mo_2C species has been reported as an active material for the methane conversion to aromatics, the thin film grown at 600 °C was studied as a catalyst for the CH_4 conversion by a micro-reactor system. The reaction profile was qualitatively recorded in Fig. 6. It can be observed that immediately with the introduction of methane, benzene (trace a) and hydrogen (trace b) were formed, indicating that dehydrogenation–aromatization takes place, and that the thin film is an active catalyst for this conversion. The signal of benzene was low as only about $4\,\mathrm{cm}^2$ of active area was involved in the test reaction. In a blank test with only Si substrate, no benzene and hydrogen was observed when introducing methane at 700 °C or above.

4. Conclusions

The following inferences can be drawn from the above results.

1. High density, well distributed nano-structured $Mo_2C(2\,2\,0)$ films were obtained from rapidly heated MOCVD using $Mo(CO)_6$ precursor at 600 °C and above. Film morphology was dependent on rapid heating rate, deposition temperature and time.
2. XPS and AES study showed that the film is composed of mainly Mo_2C with small amount of MoO_3. The reaction scheme for the film formation was proposed.
3. The thin film has shown a catalytic activity to methane conversion to aromatics.

Acknowledgements

This work is supported by ABB Lummus Global Inc.

References

[1] P.W. Jacobs, Catal. Lett. 37 (1996) 131.

[2] J.Y. Ying, in: G.C. Hadjipanayis, R.W. Siegel (Eds.), Nanophase Materials, Kluwer Academic Publishers, Dordrecht, 1994, p. 37.

[3] S.N. Goncharova, in: G. Poncelet (Ed.), Preparation of Catalysts, vol. VI, Elsevier, Amsterdam, 1995, p. 915.

[4] B.M. Weckhuysen, Catal. Lett. 52 (1998) 31.

[5] B.M. Weckhuysen, D. Wang, M.P. Rosynek, J.H. Lunsford, J. Catal. 175 (1998) 338.

[6] D. Wang, J.H. Lunsford, M.P. Rosynek, Topic Catal. 3 (1996) 289.

[7] D. Wang, J.H. Lunsford, M.P. Rosynek, J. Catal. 169 (1997) 347.

[8] C.Y. Chang, S.M. Sze (Eds.), ULSI Technology, Wiley, New York, 1996, p. 144.

[9] H. Luth, Surfaces and Interface of Solid Materials, Springer-Verlag, Berlin, 1995.

[10] F.A. Cotton, G. Wilkinson, Advanced Inorganic Chemistry, 5th ed., Wiley, 1988.

[11] JCPDS-ICDD CD-ROM Powder Diffraction Database, 1995.